Journal of Structural Geology, Vol. 15, No. 2, pp. 123 to 128, 1993
Printed in Great Britain

0191–8141/93 \$06.00+0.00

Load-strengthening versus load-weakening faulting

RICHARD H. SIBSON

Department of Geology, University of Otago, P.O. Box 56, Dunedin, New Zealand

(*Received* 3 *September* 1991; *accepted in revised form* 12 *July* 1992)

Abstract—Increases in shear stress (τ) along a fault during loading to failure cannot generally occur without changes in the normal stress across the fault (σ_n). The fault loading parameter ($\partial\sigma_n'/\partial\tau = \partial\sigma_n/\partial\tau - \partial P_f/\partial\tau$) distinguishes situations of *load-strengthening* ($\partial\sigma_n'/\partial\tau > 0$), where the frictional shear strength of faults increases as tectonic shear stress rises, from *load-weakening* environments ($\partial\sigma_n'/\partial\tau < 0$) where it decreases. Compressional faulting in tectonic regimes with $\sigma_v = \sigma_3$ is always load-strengthening unless fluid pressure is rapidly increasing. Extensional faulting in regimes where $\sigma_v = \sigma_1$ is load-weakening unless fluid pressure is dropping rapidly. Strike-slip faulting in terrains where $\sigma_v = \sigma_2$ can be either load-weakening or load-strengthening. The particular case where $\partial\sigma_n'/\partial\tau = 0$, so that frictional shear strength stays constant during fault loading, is a very special situation corresponding to direct shear. Load-strengthening strike-slip faulting appears to correlate with tectonic transpression and load-weakening with transtension. Differing loading characteristics of faults in different tectonic regimes must induce varying patterns of cyclic fluid redistribution accompanying the seismic cycle, with implications for earthquake recurrence and precursory groundwater phenomena.

INTRODUCTION

STRESS conditions for failure on different types of faults in the frictional regime of the upper crust are fairly well understood (Anderson 1951), but the stress path by which particular failure states are reached during fault loading has received less attention. Following Hubbert & Rubey (1959), the static frictional strength of an existing fault in fluid-saturated crust under triaxial stress (effective principal compressive stresses $\sigma_1' = (\sigma_1 - P_f) > \sigma_2' = (\sigma_2 - P_f) > \sigma_3' = (\sigma_3 - P_f)$), may be approximated by a criterion of Coulomb form:

$$\tau_f = C + \mu_s\sigma_n' = C + \mu_s(\sigma_n - P_f), \quad (1)$$

where C is the cohesive or cementation strength of the fault (which may be small for an active structure), μ_s is the static coefficient of friction with a typical value of ~0.75 (Byerlee 1978), P_f is the fluid pressure and σ_n is the normal stress on the fault. Reactivation of the fault occurs when the shear stress matches its frictional strength (ie. $\tau = \tau_f$) and is generally assumed to result from an increase in tectonic shear stress. However, failure may also be induced by reduction of normal stress, or by an increase in fluid pressure (as in the case of earthquakes triggered by fluid injection and reservoir impounding—see Nicholson & Wesson 1990) or through some combination of all these factors.

In block-slider models of frictional instability on faults (often employed as analogues to episodic seismic slip), failure occurs solely in response to rising shear stress as in a direct shear experiment. However, as a general rule, shear stress on faults in the Earth's crust cannot be increased without also changing the normal stress, which in turn affects the frictional strength of the fault. Normal stress is directly related to the level of mean stress ($\bar{\sigma} = [\sigma_1 + \sigma_2 + \sigma_3]/3$), affecting the *dilatation* of a rock mass, so that patterns of fluid flow during faulting are likely to be affected by the manner in which normal and mean stress change as shear stress rises on a fault. Some of the implications of these effects for earthquake recurrence have been considered by Sibson (1991).

We examine first the loading of existing faults to failure in different stress regimes within homogeneous dry crust ($P_f = 0$). Subsidiary effects are considered in relation to progressively increasing shear stress, which is regarded as the main factor involved in the loading of faults to failure in accordance with simple elastic rebound concepts. Consideration is then given to some of the effects likely to be associated with fault loading in fluid-saturated crust. No account is taken of stress inhomogeneities at fault tips or irregularities (Segall & Pollard 1980), though local stress concentrations may be expected to modify some of the fluid redistribution effects (Nur & Booker 1972). It is also assumed that fault failure occurs from simple frictional instability in accordance with the Coulomb criterion above, and not from time-dependent failure at constant stress as the result of processes such as stress corrosion (e.g. Das & Scholz 1981).

FAULT LOADING IN DRY CRUST

Taking account of the near-surface boundary condition of zero horizontal shear stress, Anderson (1951) recognized three geological stress regimes in each of which one of the three principal compressive stresses ($\sigma_1 > \sigma_2 > \sigma_3$) is vertical. In dry crust, it is apparent from equation (1) that frictional fault strength is determined by the level of normal stress which is directly coupled to the shear stress, but the nature of this coupling varies with the different Andersonian stress regimes. The vertical stress, σ_v, arising from the gravitational load of overlying rock, is assumed to stay constant through successive loading cycles. This is reasonable at all but very shallow depths, because $\Delta\sigma_v$ arising from earthquake-induced height changes amounts to only ~0.03 MPa m^{-1} of vertical displacement, which is small in comparison with shear stress drops and other stress changes accompanying earthquakes (see below).

To simplify the analysis, fault loading is considered for the special cases where the σ_2 axis is contained within the plane of the faults and its effects can be neglected. The standard two-dimensional equations for shear and normal stress on a plane lying at a reactivation angle, θ_r, to σ_1, are then:

$$\tau = 0.5(\sigma_1 - \sigma_3)\sin 2\theta_r \tag{2}$$

and

$$\sigma_n = 0.5[(\sigma_1 + \sigma_3) - (\sigma_1 - \sigma_3)\cos 2\theta_r]. \tag{3}$$

For this two-dimensional analysis, mean stress may be written $\bar{\sigma} = 0.5(\sigma_1 + \sigma_3)$, so that equations (2) and (3) combine to give:

$$\bar{\sigma} = \sigma_n + \tau \cot 2\theta_r \tag{4}$$

relating normal, mean and shear stresses for a particular fault orientation. The relationship between changes in normal stress and mean stress with varying τ is therefore given by:

$$\partial\bar{\sigma}/\partial\tau = \partial\sigma_n/\partial\tau + \cot 2\theta_r. \tag{5}$$

Dip-slip faulting

In a compressional regime with constant vertical stress, $\sigma_v = \sigma_3$, equations (2) and (3) yield:

$$\sigma_n = \sigma_v + \tan\theta_r\,\tau. \tag{6}$$

From equations (1) and (6), the relationship between changes in shear stress and the change in frictional strength of a reverse fault is:

$$\Delta\tau_f = \mu_s\Delta\sigma_n = \mu_s\tan\theta_r\,\Delta\tau \tag{7}$$

and, in dry crust, the loading parameter is $\partial\sigma_n/\partial\tau = \tan\theta_r$. This parameter remains positive for all values of $\theta_r < 90°$ so that reverse fault loading in dry crust is always *load-strengthening*. Changes in mean stress are related to changes in shear stress by:

$$\Delta\bar{\sigma} = \Delta\tau/\sin 2\theta_r. \tag{8}$$

Note that loading of reverse faults to failure in dry crust is only possible if $\partial\tau_f/\partial\tau < 1$, requiring $\theta_r < \tan^{-1}(1/\mu_s)$, the angle of frictional lock-up (Sibson 1985, 1990). For $\mu_s = 0.75$, the lock-up angle is ~53°.

Within an extensional regime where $\sigma_v = \sigma_1$, the equations for stress on a plane yield:

$$\sigma_n = \sigma_v - \cot\theta_r\,\tau \tag{9}$$

so that changes in frictional strength and shear stress are related by:

$$\Delta\tau_f = -\mu_s\cot\theta_r\,\Delta\tau \tag{10}$$

and the loading parameter, $\partial\sigma_n/\partial\tau = -\cot\theta_r$. Loading of normal faults to failure in dry crust is therefore *load-weakening*. Changes in mean stress are then given by:

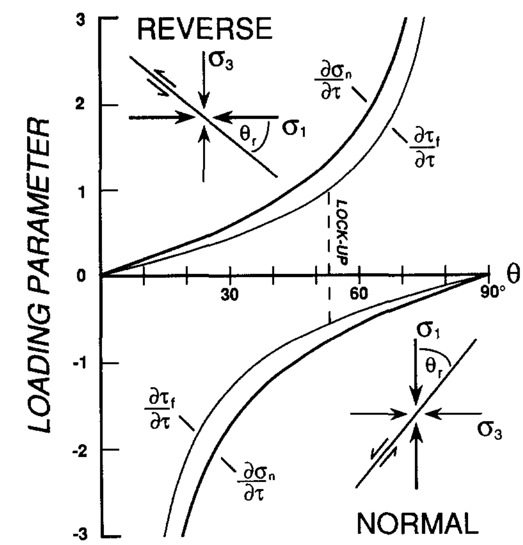

Fig. 1. Loading parameter, $\partial\sigma_n/\partial\tau$, and $\partial\tau_f/\partial\tau$ plotted against fault reactivation angle (θ_r) for pure reverse and normal dip-slip faults in dry crust where σ_v is, respectively, σ_3 and σ_1. Dotted line represents the reactivation angle where frictional lock-up will occur.

$$\Delta\bar{\sigma} = -\Delta\tau/\sin 2\theta_r. \tag{11}$$

Thus, for pure dip-slip faulting in dry crust with constant vertical stress, both $\partial\sigma_n/\partial\tau$ and $\partial\bar{\sigma}/\partial\tau$ depend solely on the dip of the faults (Fig. 1). Both have positive values in compressional regimes (*load-strengthening*) and negative values in extensional regimes (*load-weakening*). Figure 2(a) illustrates the progressive loading to failure of cohesionless reverse and normal faults that are optimally oriented for frictional reactivation ($\theta_r = 0.5\tan^{-1}(1/\mu_s) \approx 27°$ for $\mu_s = 0.75$), with $\partial\sigma_n/\partial\tau$, respectively, greater and less than zero. The relationships between shear stress, frictional fault strength and mean stress during fault loading have been plotted for a depth of 1 km in dry crust (Fig. 3), illustrating the contrast between *load-strengthening* and *load-weakening* dip-slip faulting. Loading to failure is assumed to occur from an initial state of lithostatic stress ($\sigma_v = \sigma_1 = \sigma_2 = \sigma_3 \approx 26$ MPa) (Anderson 1951, McGarr 1988) with frictional failure accompanied by a drop in shear stress, $\Delta\tau$.

Strength changes after failure

For load-strengthening faults, dropping shear stress at failure is accompanied by a decrease in the static frictional strength (Fig. 3). However, for load-weakening faults, the paradoxical situation arises that the drop in shear stress at failure is accompanied by an increase in the frictional strength of the fault. At first sight, this might be expected to prevent progressive failure. $\Delta\tau_f$ is, however, the static change in frictional strength that has occurred at the end of dynamic fault rupture, which starts at a point and spreads over a fault surface. Dynamic friction during rupture may depend on factors other than normal stress.

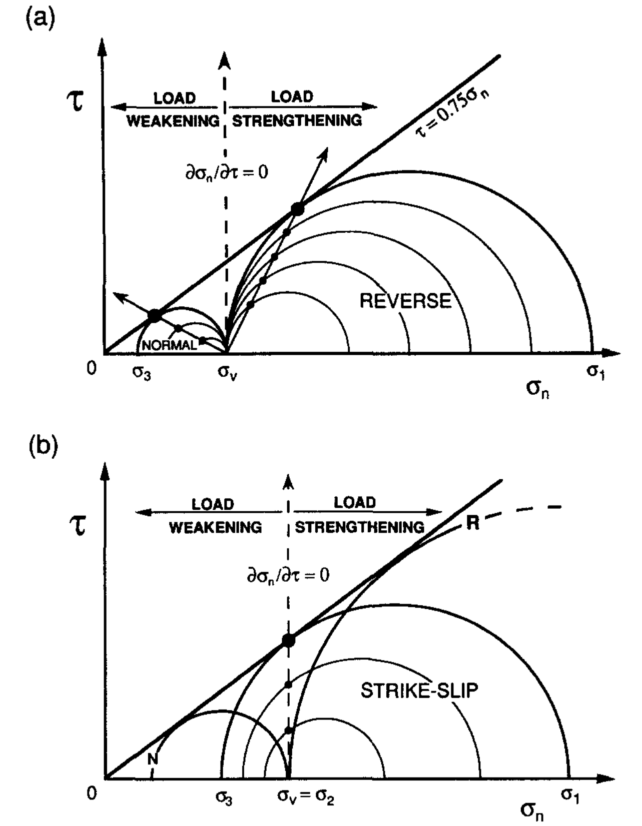

Fig. 2. (a) Mohr diagram showing progressive loading to failure of optimally oriented cohesionless reverse and normal faults with μ_s = 0.75 from an initial lithostatic stress state ($\sigma_v = \sigma_1 = \sigma_2 = \sigma_3$) in dry crust illustrating fields of load-strengthening and load-weakening. (b) Loading to failure of an optimally oriented cohesionless strike-slip fault in dry crust from an initial lithostatic stress state. The special case of progressive loading where $\partial\sigma_n/\partial\tau = 0$ (corresponding to direct shear) is illustrated. N and R represent the end-member stress states for strike-slip loading.

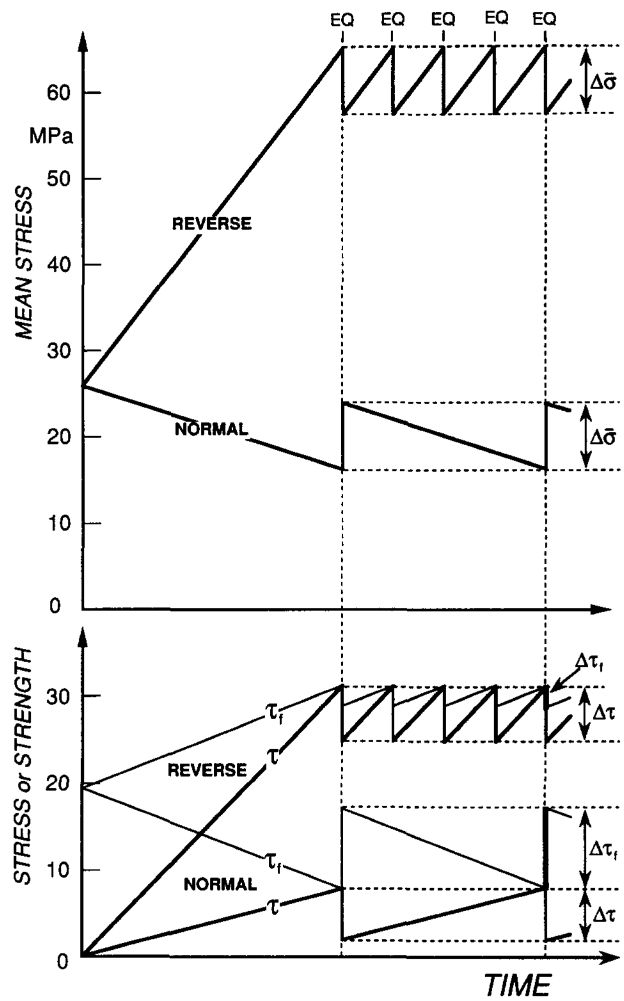

Fig. 3. Plot of stress and strength vs time illustrating the coupled relationships between tectonic shear stress (τ), frictional fault stength (τ_f) and mean stress ($\bar{\sigma}$) during cyclic loading to failure of optimally oriented cohesionless reverse and normal dip-slip faults with μ_s = 0.75 at 1 km depth in dry crust. Initial stress state is lithostatic ($\sigma_v = \sigma_1 = \sigma_2 = \sigma_3 \approx 26$ MPa); shear stress drop at failure is arbitrarily selected as $\Delta\tau$ = 6 MPa, staying constant for successive failure events.

Strike-slip faulting

The loading of strike-slip faults ($\sigma_v = \sigma_2$) is much less constrained (Fig. 2b). End-member situations arise when σ_1 increases from an initial lithostatic stress state with σ_3 held constant (corresponding to reverse fault loading, R), and when σ_3 decreases progressively with σ_1 held constant (corresponding to normal fault loading, N). An infinite range of possible stress loading schemes lies between these end-member cases for optimally oriented strike-slip faults. Moreover, it is apparent from equation (5) that there are some loading paths for strike-slip faults where load-strengthening is accompanied by a reduction in mean stress, or load-weakening by an increase.

Figure 2(b) illustrates the particular case where normal stress on an optimally oriented fault stays constant as ($\sigma_1 - \sigma_3$) and τ progressively increase to failure, so that $\partial\sigma_n/\partial\tau = 0$. This corresponds to a direct shear experiment where normal stress on a sliding surface is held constant while shear and mean stress increase during loading. Direct shear loading therefore separates load-strengthening from load-weakening strike-slip faults in dry crust.

These different strike-slip loading conditions may be considered with regard to transpressive and transtensile tectonic settings, which are usually defined on kinematic grounds or in terms of the finite strains associated with transform plate boundaries (Harland 1971, Sanderson & Marchini 1984, Sylvester 1988). Fault configurations may, however, change with time relative to plate motions and regional stress fields. Because transpression is usually associated with subsidiary reverse faulting and transtension with normal faulting, these different tectonic environments appear to equate with load-strengthening and load-weakening systems of strike-slip loading, respectively. This provides a useful means for discriminating transpression and transtension on strike-slip faults during the loading cycle leading to a single increment of fault slip.

FAULT LOADING IN FLUID-SATURATED CRUST

In fluid-saturated crust, normal and mean stress remain linked to shear stress by the relationships previously outlined for the different loading environments.

However, because P_f may be affected by changes in mean stress, frictional shear strength (depending on effective normal stress) no longer depends directly on shear stress. In these circumstances, the fault loading parameter may be generalized to:

$$\partial\sigma_n'/\partial\tau = \partial\sigma_n/\partial\tau - \partial P_f/\partial\tau \qquad (12)$$

which again serves to distinguish between situations of *load-strengthening* ($\partial\sigma_n'/\partial\tau > 0$) and *load-weakening* ($\partial\sigma_n'/\partial\tau < 0$).

Several factors complicate analysis of fluid redistribution during cyclic loading. For a start, basic knowledge of permeability values in the vicinity of active fault zones at depths of more than a few kilometres is generally lacking. Fracture permeability probably predominates, especially in crystalline rocks, but is likely to be very heterogeneous. Given the roughness of rupture surfaces (Power *et al.* 1987), post-failure permeability in the immediate vicinity of fault zones is also likely to be substantially greater than that existing pre-failure. Additionally, in evaluating fluid redistribution with respect to the earthquake stress cycle, several different time scales have to be considered: the long-term accumulation of shear stress through the interseismic period lasting tens to perhaps many thousands of years, the rapid stress drop during seismic rupture which at any one place occurs over a period of a few seconds, and the period of post-seismic adjustment and aftershock activity lasting for days to years depending on the size of the rupture.

Full evaluation of time-dependent, poroelastic effects in fluid saturated crust would require a thorough knowledge of the spatial variation of elastic and hydraulic properties, and would also take account of stress inhomogeneities at fault irregularities and rupture tips (Nur & Booker 1972, Rice & Cleary 1976). Nothing more than a qualitative evaluation of likely loading-related effects in uniform crust is attempted here. We also assume that fluid redistribution is governed solely by changing mean stress, taking no account of effects that might arise from the different varieties of shear stress-dependent dilatancy that may be important in faulting (e.g. Nur 1975).

Extent of zone affected by stress cycling

The analysis till now has been for stress changes associated with rupturing on an infinite fault in uniform crust, which would lead to a homogeneous change in the state of stress. In practice, the finite size of earthquake ruptures limits the areal extent of stress cycling so that, neglecting stress concentrations at rupture tips, the amplitude of the shear stress change diminishes with increased distance from the fault (e.g. Mavko 1981). Dimensions of the region affected by significant stress cycling are broadly comparable to characteristic rupture dimensions, perhaps extending laterally for distances of 10–15 km from ruptures that occupy the full depth of the continental seismogenic zone.

While the magnitude of shear stress driving earthquake faulting remains uncertain (Hanks & Raleigh 1980), the drop in shear stress during an earthquake, averaged over the rupture surface, is generally in the range $1 < \Delta\tau < 10$ MPa (Kanamori & Anderson 1975). From equations (8) and (11), corresponding changes in mean stress for dip-slip faulting depend on fault dip, but are at least as large as the shear stress drop. Expressed in terms of equivalent hydraulic head, the corresponding range for $\Delta\bar{\sigma}$ would extend from >100 to >1000 m. By creating lateral gradients in hydraulic head, variations in mean stress during loading are therefore likely to induce significant fluid redistribution in the area around an active fault that undergoes stress cycling.

Interseismic period

Consider first the situation where the crust around an active fault remains sufficiently well-drained that fluid pressure remains more or less constant as mean stress varies through the interseismic period. This is the situation likely to prevail in highly fractured and hydrostatically pressured portions of the uppermost crust. As an initial condition, the region affected by the shear stress drop of a ruptured fault is considered at a time post-failure when any fluid pressure transients arising from the earthquake have relaxed back to hydrostatic equilibrium. The greatest changes in the levels of shear and mean stress during loading to the next failure event will occur immediately adjacent to the fault. Thus in a compressional regime, where load-strengthening is accompanied by rising mean stress, fluids will tend to move laterally away from the fault through the interseismic period. However, fluids will tend to migrate laterally inward towards faults undergoing load-weakening with progressively decreasing mean stress. Provided fluid pressure stays constant during loading, the simple coupling relationships between changes in shear stress and frictional shear strength (equations 7 and 10) remain unaffected.

If, on the other hand, the permeability around a fault is too low to permit drainage on the time scale of the interseismic interval, rising mean stress around a load-strengthening fault will cause a local increase in fluid pressure, retarding the coupled increase in frictional strength (Fig. 3) and decreasing time to failure (cf. Cello & Nur 1988). In contrast, fluid pressure around a load-weakening fault may drop as mean stress decreases so that the rate of strength reduction during loading diminishes and the time to failure increases. Fluid migration driven by fault loading in imperfectly drained crust may thus exert a considerable influence on recurrence behaviour (Sibson 1991).

Pre-seismic effects

If rupturing on a fault is anticipated by a phase of accelerating aseismic slip as studies of frictional instability suggest (e.g. Dieterich 1986), any precursory relaxation of shear stress should be accompanied by a reversal in the pattern of fluid migration around the

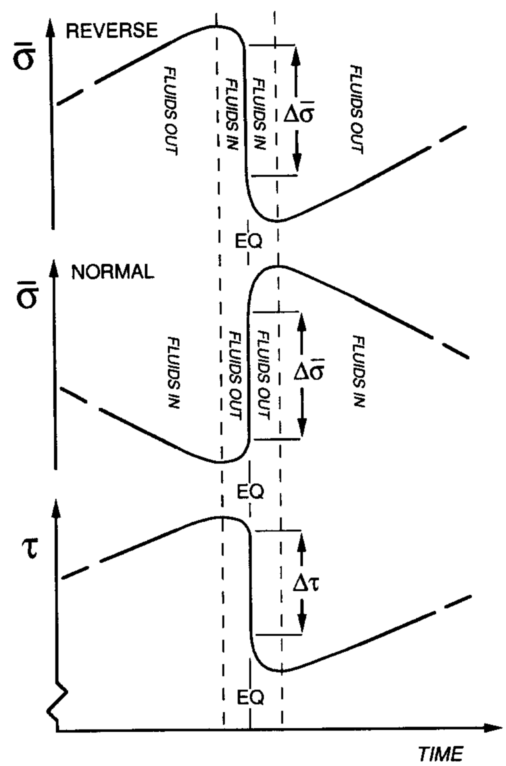

Fig. 4. Coupled relationships between shear stress, τ, and mean stress, $\bar{\sigma}$, on optimally oriented reverse and normal faults, illustrating expected changes in fluid migration accompanying pre-seismic and post-seismic slip.

fault. This is illustrated for reverse and normal dip-slip faults in Fig. 4. Such short-term flow reversals may contribute to the premonitory groundwater effects sometimes observed immediately before shallow crustal earthquakes (Roeloffs 1988), but the effects will be diametrically opposite for load-strengthening and load-weakening faults.

Coseismic and post-seismic effects

Sudden changes in mean stress accompanying the shear stress drop at failure should lead to an instantaneous response approximating that of undrained material. Changes in fluid pressure will partly counteract the changes in mean stress, thereby diminishing instantaneous changes in shear strength (Nur & Booker 1972, Rice & Cleary 1976). Fluid infiltration of the instantaneously underpressured zone around load-strengthening faults from the surrounding region then causes time-dependent post-failure weakening. In the vicinity of normal faults, drainage of the instantaneous overpressures induced at failure must lead to a progressive strengthening of the fault. The general effect of pore fluids, therefore, is to delay the strength changes at failure predicted by the 'dry fault' analysis.

Fluid-pressured failure

Provided the fluid content of the rock mass stays constant, changes in fluid pressure through coupled poroelasticity will in general only partly counteract changes in mean stress (Rice & Cleary 1976). However, it is apparent from equation (12) that fluid ingress from an external source, leading to increased fluid pressure in the vicinity of a fault, could yield $\partial\sigma_n'/\partial\tau < 0$, even though $\partial\sigma_n/\partial\tau > 0$. A rapid build-up of fluid pressure could therefore induce load-weakening in a compressional–transpressional tectonic environment which would otherwise be load-strengthening. In contrast, increasing fluid pressure in extensional–transtensional settings would accelerate load-weakening to failure.

These results have application to the artificial triggering of fault failure through fluid injection (Nicholson & Wesson 1990), which is essentially a load-weakening process, and perhaps also to some natural faulting. At least some intraplate earthquakes seem likely to be triggered by natural localized increases in fluid-pressure, particularly those occurring on faults that are severely misoriented for frictional reactivation in compressional regimes (Sibson 1990). The converse situation, where a rapid decrease in fluid pressure counteracts load-weakening in extensional–transtensional regimes and leads to load-strengthening, seems less likely to be important for natural faulting.

DISCUSSION

The contrasting loading of faults in different tectonic settings has a broad range of implications, as yet only partly explored. To begin with, contrasting changes in shear strength during the loading to failure of thrust and normal faults suggest that they should be characterized by entirely different styles of pre- and post-failure behaviour, perhaps reflected in contrasting patterns of foreshock and aftershock activity, and fluid redistribution. However, these factors do not appear to have been considered in recent comparative studies of aftershock activity (e.g. Kisslinger & Jones 1991) or fluid redistribution (Roeloffs 1988).

In terms of pre-seismic and post-seismic behaviour, the differing effects on groundwater redistribution are likely to be especially important. An example of an effect attributable to the coupled increase in mean stress accompanying normal fault failure was observed immediately following the 1983 $\mathbf{M}_s$7.3 Borah Peak earthquake in Idaho, when groundwater fountained violently from bedrock fissures striking parallel to the rupture trace (Wood *et al.* 1985). Subvertical extensional hydrofractures are likely to develop under hydrostatic fluid pressures close to the surface in the pre-failure deviatoric stress field around normal faults (Sibson 1981). Such near-instantaneous expulsion of fluids can be attributed to the increase in horizontal σ_3 post-failure, forcing the closure of such hydrofractures (cf. Carrington *et al.* 1991).

Where fluid redistribution occurs through the fault loading cycle as a consequence of changing mean stress, recurrence intervals between successive earthquakes in fluid-saturated crust are unlikely to depend solely on the rate of shear stress (and strain) accumulation as is commonly supposed (Shimazaki & Nakata 1980). In such circumstances, the time-dependence of frictional shear strength is affected by pore fluid migration as well as by coupling to shear stress. Because fluid flux through fracture networks is highly sensitive to fracture aperture (Norton & Knapp 1977), which may be affected by hydrothermal dissolution and/or cementation and other processes, the rate and volume of fluid migration may vary significantly from one seismic loading cycle to the next, affecting the time-dependence of frictional strength and the regularity of recurrence (Sibson 1991).

Apart from its significance with respect to earthquake recurrence and precursory behviour, redistribution of fluids accompanying fault loading is also likely to play an important role in mineralization. Cyclic passage of hydrothermal fluids adjacent to faults in response to changing mean stress may contribute to disseminated mineralization in fractured rock masses. Though the process could operate to some extent at all levels of the seismogenic zone, it seems likely to be particularly effective in highy fractured rock at high crustal levels where background fluid pressures are close to hydrostatic.

It should be borne in mind, however, that situations may arise where the strength changes resulting from the coupling between normal and shear stresses may be subordinated by other processes. Fluid redistribution may also be affected by the different forms of shear stress dependent dilatancy described by Nur (1975). Another masking process would be large interseismic strength changes arising from *fault-valve* behaviour, when rupturing occurs in crust that is strongly fluid overpressured and postfailure flushing of the overpressured system along the rupture zone leads to a large increase in fault strength. Valving action of this kind is especially likely in compressional regimes, and may be prevalent in the deeper levels of the seismogenic zone where larger ruptures nucleate (Sibson 1990).

Acknowledgements—Research leading to this paper was supported by National Science Foundation grant EAR89-04571. I thank Win Means, Art McGarr, Richard Norris, Jim Rice, Chris Scholz and an anonymous reviewer for helpful comments and discussion on the manuscript.

REFERENCES

Anderson, E. M. 1951. *The Dynamics of Faulting and Dyke Formation with Applications to Britain* (2nd edn). Oliver & Boyd, Edinburgh.

Byerlee, J. D. 1978. Friction of rocks. *Pure & Appl. Geophys.* **116**, 615–626.

Carrington, C. R., King, G. C. P., Barr, G. E. & Bixter, N. E. 1991. Potential for water-table excursions induced by seismic events at Yucca Mountain, Nevada. *Geology* **19**, 1157–1160.

Cello, G. & Nur, A. 1988. Emplacement of foreland thrust systems. *Tectonics* **7**, 261–271.

Das, S. & Scholz, C. H. 1981. Theory of time-dependent rupture in the earth. *J. geophys. Res.* **86**, 6039–6051.

Dieterich, J. H. 1986. A model for the nucleation of earthquake slip. In: *Earthquake Source Mechanics* (edited by Das, S., Boatwright, J. & Scholz, C. H.). *Am. Geophys. Un. Maurice Ewing Series* **6**, 38–47.

Hanks, T. C. & Raleigh, C. B. 1980. The conference on magnitude of deviatoric stresses in the Earth's crust and uppermost mantle. *J. geophys. Res.* **85**, 6083–6085.

Harland, W. B. 1971. Tectonic transpression in Caledonian Spitsbergen. *Geol. Mag.* **108**, 27–42.

Hubbert, M. K. & Rubey, W. W. 1959. Role of fluid pressure in the mechanics of overthrust faulting. *Bull. geol. Soc. Am.* **58**, 362–375.

Kanamori, H. & Anderson, D. L. 1975. Theoretical basis of some empirical relations in seismology. *Bull. seism. Soc. Am.* **65**, 1073–1096.

Kisslinger, C. & Jones, L. M. 1991. Properties of aftershock sequences in southern California. *J. geophys. Res.* **96**, 11,947–11,958.

Mavko, G. M. 1981. Mechanics of motion of major faults. *Annu. Rev. Earth. & Planet. Sci.* **9**, 81–111.

McGarr, A. 1988. On the state of lithospheric stress in the absence of applied tectonic forces. *J. geophys. Res.* **93**, 13,609–13,617.

Nicholson, C. & Wesson, R. L. 1990. Earthquake hazard associated with deep well injection—a report to the U.S. Environmental Protection Agency. *Bull. U.S. geol. Surv.* **1951**.

Norton, D. & Knapp, R. 1977. Transport phenomena in hydrothermal systems: the nature of porosity. *Am. J. Sci.* **277**, 918–936.

Nur, A. 1957. A note on the constitutive law for dilatancy. *Pure & Appl. Geophys.* **113**, 197–206.

Nur, A. & Booker, J. 1972. Aftershocks caused by pore-fluid flow? *Science* **175**, 885–887.

Power, W. L., Tullis, T. E., Brown, S., Boitnott, G. N. & Scholz, C. H. 1987. Roughness of natural fault surfaces. *Geophys. Res. Lett.* **14**, 29–32.

Rice, J. R. & Cleary, M. P. 1976. Some basic stress diffusion solutions for fluid-saturated elastic porous media with compressible constituents. *Rev. Geophys. & Space Phys.* **14**, 227–241.

Roeloffs, E. A. 1988. Hydrological precursors to earthquakes: a review. *Pure & Appl. Geophys.* **126**, 177–209.

Sanderson, D. J. & Marchini, W. R. D. 1984. Transpression. *J. Struct. Geol.* **6**, 449–458.

Segall, P. & Pollard, D. D. 1980. Mechanics of discontinuous faults. *J. geophys. Res.* **85**, 4337–4350.

Shimazaki, K. & Nakata, T. 1980. Time-predictable recurrence model for large earthquakes. *Geophys. Res. Lett.* **7**, 279–282.

Sibson, R. H. 1981. Fluid flow accompanying faulting: field evidence and models. In: *Earthquake Prediction: An International Review* (edited by Simpson, D. W. & Richards, P. G.). *Am. Geophys. Un. Maurice Ewing Series* **4**, 593–603.

Sibson, R. H. 1985. A note on fault reactivation. *J. Struct. Geol.* **7**, 752–754.

Sibson, R. H. 1990. Rupture nucleation on unfavorably oriented faults. *Bull. seism. Soc. Am.* **80**, 1580–1604.

Sibson, R. H. 1991. Loading of faults to failure. *Bull. seism. Soc. Am.* **81**, 2493–2497.

Sylvester, A. G. 1988. Strike-slip faults. *Bull. geol. Soc. Am.* **100**, 1666–1703.

Walder, J. S. & Nur, A. 1984. Porosity reduction and crustal pore fluid development. *J. geophys. Res.* **89**, 11,539–11,548.

Wood, S. H., Wurts, C., Ballenger, N., Shaleen, M. & Totorica, D. 1985. The Borah Peak, Idaho earthquake of October 28, 1983—hydrologic effects. *Earthquake Spectra* **2**, 127–150.